

Hosing and Sloshing of Short-Pulse GeV-Class Wakefield Drivers

E. S. Dodd, R. G. Hemker, C.-K. Huang, S. Wang, C. Ren, and W. B. Mori

University of California, Los Angeles, Los Angeles, California 90095

S. Lee and T. Katsouleas

University of Southern California, Los Angeles, California 90089

(Received 12 February 2001; revised manuscript received 25 September 2001; published 7 March 2002)

This Letter examines the electron-hosing instability in relation to the drivers of current and future plasma-wakefield experiments using fully three-dimensional particle-in-cell simulation models. The simulation results are compared to numerical solutions and to asymptotic solutions of the idealized analytic equations. The measured growth rates do not agree with the existing theory and the behavior is shown to depend sensitively on beam length, shape, and charge. We find that even when severe hosing occurs the wake can remain relatively stable.

DOI: 10.1103/PhysRevLett.88.125001

PACS numbers: 52.40.Mj, 41.75.Lx, 52.65.Rr

Plasma wakefield accelerators (PWFA) are the subject of much current research, because of the large accelerating gradients they may produce. In the blowout regime of the PWFA [1], where the spot size is small compared to a skin depth ($\sigma_{\perp} \ll c/\omega_p$) and the peak beam density exceeds the plasma density ($n_b \gg n_0$), the wake has large accelerating fields and ideal focusing forces. If the bunch has a head-tail offset, the focusing force will cause the tail to realign behind the head, thus oscillating transversely, ringing (sloshing) from the realignment. Under certain conditions this oscillation will grow exponentially due to the electron beam hosing instability [2,3]. This has ramifications for existing PWFA experiments, including Ref. [4] and E-157 at the Stanford Linear Accelerator (SLAC) [5] where the goal is to detect the acceleration of the back of the bunch. This sloshing of the tail and any amplification of it (i.e., hosing) could complicate the interpretation and analysis of an experiment. Moreover, future PWFA designs for higher energies and longer plasmas will be even more prone to the hose instability according to current theory.

The hosing instability and the closely related transverse two-stream instability (when $n_b < n_0$) have been studied previously with both theory [2,6–11] and computer simulation [3,8–10], and is similar to the beam-breakup instability in conventional accelerators [12]. The existing theory predicts that hosing will occur for the parameters of the E-157 experiment, but simulations in this Letter show little or no growth. Results from the E-157 experiment also indicate little or no growth [13]. However, our simulations do show that the instability does occur, but at a reduced growth rate from existing theory for: a longer pulse length; a wedge-shaped beam; and for higher-beam charge. Therefore, the existing theory, developed for beams propagating in preformed or adiabatically formed channels, is in need of modification. Understanding hosing in the nonadiabatic limit, where the pulse rise time and length are short or comparable to the plasma period, is the main point of this Letter. Recently, in Ref. [14] the nonadiabatic limit was also studied with a reduced description code. Through compari-

sons with OSIRIS results to our own similar code, we show that the reduced particle-in-cell overestimates the amount of hosing growth. In addition we compare these with the theoretical predictions and discuss the consequences of hosing to the wake.

We begin by describing what the existing theory [2] predicts. The channel's centroid is x_c and x_b is the beam centroid. When the beam has an initial head-tail offset, the channel forms behind the front of the pulse. The previous work [2] has shown that the instability is described by the two coupled harmonic oscillator equations:

$$\partial_s^2 x_b + k_{\beta}^2 x_b = k_{\beta}^2 x_c, \quad (1)$$

$$\partial_{\xi}^2 x_c + \omega_0^2 x_c = \omega_0^2 x_b. \quad (2)$$

Here, the equations are written in the moving frame of the beam, with $\xi = z - ct$ and $s = z$. In these equations we see that the beam centroid x_b is driven by the channel centroid x_c , and vice versa. The frequency of oscillation along the length of the beam is $\omega_0 = \omega_p/\sqrt{2}c$ and the beam's tail will oscillate transversely at the betatron frequency $k_{\beta} = \omega_p/\sqrt{2}\gamma c$, where ω_p is the plasma frequency and γ is the relativistic factor of the electrons.

There is no closed analytic solution to Eqs. (1) and (2), however they may be integrated numerically. Asymptotic solutions to these equations exist [14], and for a short bunch ($k_{\beta}s \gg \omega_0\xi$) with a linear offset it is $x_b(s, \xi) = 0.341x_{b0}(\xi)e^A \cos(k_{\beta}s - A/\sqrt{3} + \pi/4)/A^{3/2}$, where $A(s, \xi) = 3^{3/2}[(k_{\beta}s)(\omega_0\xi)^2]^{1/3}/4$, and $x_{b0}(\xi)$ is the displacement of the beam at $s = 0$. To illustrate the possible importance of hosing, we consider the parameters in the E-157 experiment. The electron beam has a longitudinal Gaussian envelope $n_b(\xi) \propto \exp(\xi^2/2\sigma_{\xi}^2) \exp(r^2/2\sigma_r^2)$ with $\sigma_{\xi} = 630 \mu\text{m}$ ($1.72 c/\omega_p$), a plasma density of $n_0 = 2.1 \times 10^{14} \text{ cm}^{-3}$, and a beam energy of 30 GeV ($\gamma = 60000$). Sample integrations for these parameters with $x_c(\xi, 0) = 0$, $x_b(\xi, 0) = 0.011\omega_0\xi$, and $\partial_s x_c(\xi, 0) = \partial_s x_b(\xi, 0) = 0$ are shown in Fig. 1(a) for a point at $\xi = \sigma_{\xi}$ ($\omega_0\xi = 1.22$) behind the front of the

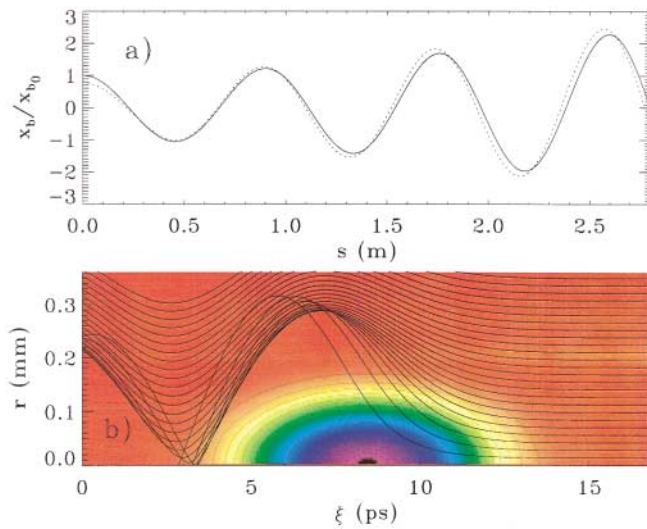


FIG. 1 (color). (a) Numeric (solid) and asymptotic (dashed) integration of the model equations for the E-157 experiment. (b) The sheet model shows the highly nonuniform channel formed by a Gaussian pulse.

channel, and plotted as a function of the propagation distance. Both the integration of Eqs. (1) and (2) (solid line) and the asymptotic solution (dashed line), show amplification of the initial offset. Here we see that after 1.4 m ($k_\beta s = 11.0$) of propagation the offset has grown by a factor of 1.5, and after 2.8 m more than doubled.

Before presenting the simulation results, it is worth describing the time scale for the formation of the channel in the nonadiabatic, short-pulse limit. We use a “sheet model” in which each electron is a ring of charge [15]. The response of these rings due to the beam’s space charge and plasma ions is calculated under the assumption that the rings do not cross and the drive beam does not evolve. In Fig. 1(b) the results of such a model are plotted for the Gaussian profile previously mentioned with a peak density of $n_b/n_0 = 3.6$. Each black line is the trajectory of a ring as it moves past the beam, thus showing that the channel forms near the center of the beam and is not uniform, but highly curved. If the beam had more charge so that $n_b/n_0 \gg 1$, then the channel forms near where $n_b/n_0 \sim 1$. This plot shows that the zeroth order channel is a dynamic function of ξ , so to lowest order $k_\beta \sim k_\beta(\xi)$.

To accurately test hosing for short electron pulses, we performed a series of self-consistent simulations using OSIRIS, which is an object-oriented particle-in-cell code capable of running in one, two, or three dimensions [16]. It is charge conserving, fully relativistic, and parallelized. The typical run had $88 \times 40 \times 20$ cells, with eight electrons per cell. The physical system was a box, $(17.6 \times 4 \times 4)c/\omega_p$ with metallic boundaries, containing a plasma density of $2.1 \times 10^{14} \text{ cm}^{-3}$, and a beam with total charge of 1.8×10^{10} electrons at 30 GeV ($\gamma = 60000$). The beam had a Gaussian shape with $\sigma_\xi = 630 \mu\text{m}$ and $\sigma_r = 70 \mu\text{m}$, an emittance of $15 \pi \text{ mm} \cdot \text{mrad}$, and a peak density of $n_b = 1.75n_0$. The instability seed was a transverse tilt in the beam with a magnitude of $10 \mu\text{m}$ at σ_ξ .

Figure 2 shows the beam’s charge density, integrated along the x_3 dimension for three different cases. The initial beam, with a tilt, is shown in Fig. 2(a); as time is advanced it will move to the right and enter the plasma. In Fig. 2(b), a beam without a tilt has propagated 1.4 m and pinched to a smaller spot size due to the betatron motion, but shows no transverse motion without the initial offset. The pulse length has shortened because the defocusing region has clipped the end off. Since $n_b < n_0$ at the front, then incomplete blowout results leading to nonuniform focusing forces, i.e., k_β is a function of ξ . The resulting phase mixing at the front of the pulse (due to the transverse two-stream instability [10]) can reduce the growth. Once a tilt is added to the beam, the back of the pulse oscillates transversely, as seen in Fig. 2(c). The tail now points upward, flipped from initially pointing downward as in Fig. 2(a). The blowout of background electrons is plotted in Fig. 2(d), where a slice is taken from the full 3D charge density. The edge of the channel can clearly be seen to be curved, as previously shown in Fig. 1(b).

In order to quantitatively measure hosing, the centroid of the beam is calculated from slices in x_2 and finding the charge weighted average position. Fig. 3(a) shows the centroid at $s = 1.4$ m scaled to the initial offset at each point. The numerical solutions to Eqs. (1) and (2) are plotted as a solid line, and show much greater growth than observed in the simulation. This numerical solution was calculated by integrating back from the position of initial complete blowout, $\xi = 11$ ps, with $x_c(\xi, 0) = 8 \mu\text{m}$. The gap from 5–7 ps corresponds to the wake’s defocusing

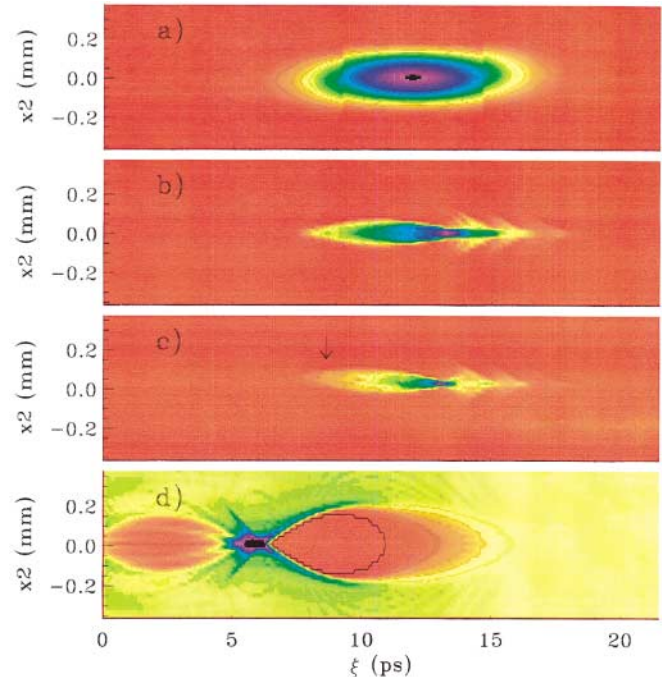


FIG. 2 (color). Charge density plots of a $\sigma_\xi = 630 \mu\text{m}$ (2 ps) pulse. (a) Initial beam with a $10 \mu\text{m}$ tilt at σ_ξ . (b) The beam without a tilt at 1.4 m. (c) The beam with a tilt at 1.4 m. (d) The channel formed by the beam.

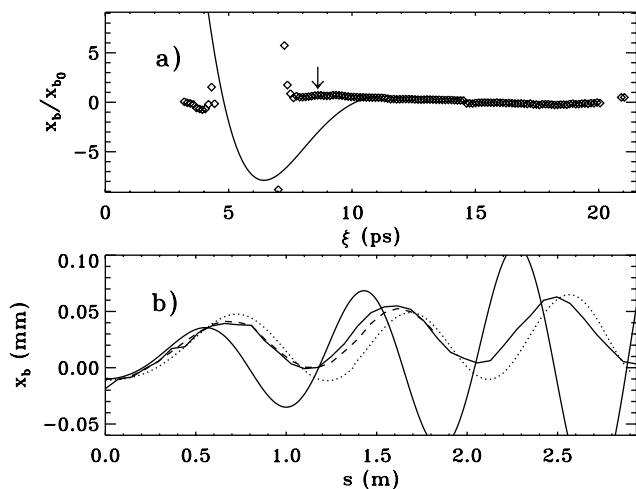


FIG. 3. The points in (a) are the calculated centroid from Fig. 2(c), overplotted with a solid line integrated from Eqs. (1) and (2). The point marked by the arrow is plotted versus time in (b). A numerical integration of the theory equations and results from the quasistatic PIC code are also shown.

region. A point was chosen near the back of the beam (arrow), where hosing should be largest. The centroid at this point is plotted as a function of propagation distance in Fig. 3(b) as a solid line. Plotted over this is a dashed line for the centroid of a higher resolution run, with $352 \times 80 \times 80$ cells and 4 particles per cell, but the same physical dimensions. Since the results differ only slightly, one assumes they are independent of resolution. (We find that in the blowout regime the cell size need not completely resolve the beam's spot size.) The centroid for the tilted beam clearly oscillates. Also, the average tail position is seen to gradually move upward, aligning behind the front of the beam. In addition, we plot the solution to Eqs. (1) and (2) by integrating back from the 11 ps position. Clearly, the simulations show little or no hosing growth when compared against the theoretical curve.

Since no hosing was seen, the next obvious step is to find conditions where it does occur. From the asymptotic solution at points further along the pulse there should be a greater amplification of the initial offset. Therefore, a simulation was run with a beam length four times longer, and four times as many electrons to keep the same peak density. All other parameters remained the same. The results are plotted in Fig. 4(a), and it is now obvious from the charge density plot that hosing has occurred. From the front to about the middle of the beam, we see the characteristic shape of hosing, while the back of the beam has actually broken apart. The breaking up of the back is mostly due to the defocusing fields of the plasma wave wake and not any hosing growth. We can conclude from this that hosing does occur, but at a reduced growth rate thus requiring a longer beam for the instability to grow.

Based on one-dimensional theory, wedge-shaped driver beams were proposed as a way to increase the transformer ratio [17]. However, in three dimensions, such a bunch shape will adiabatically expel the plasma electrons, which

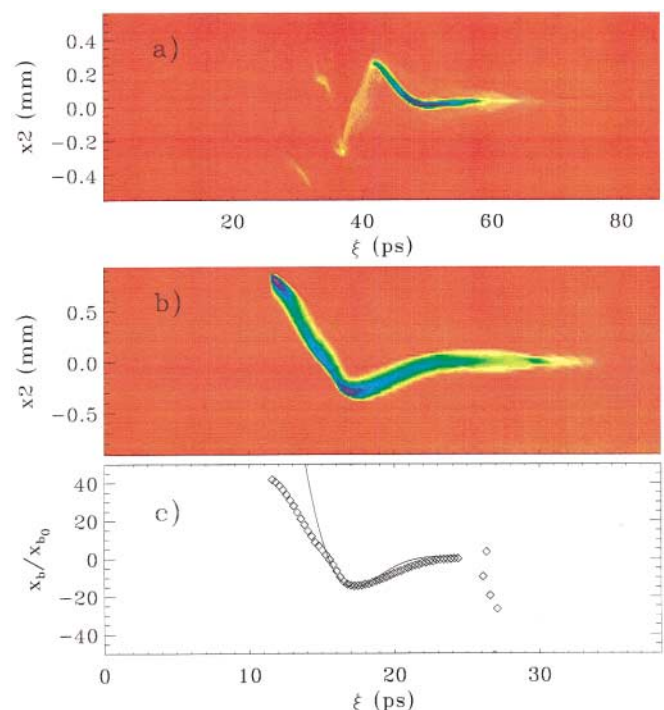


FIG. 4 (color). A Gaussian beam with $\sigma_\xi = 2520 \mu\text{m}$ (8 ps) is plotted in (a) after 1.4 m. (b) shows a wedge-shaped beam at $k_\beta s = 12.5$. (c) shows the calculated centroid compared with a numerical solution from Eqs. (1) and (2).

will not rush back until the back of the bunch has passed. Therefore, the idealized hosing theory should apply better for this situation. The stability of wedge-shaped drivers was studied in earlier simulation work [3]. However, no direct comparison to theory was given. Figure 4(b) shows the charge density plot for a pulse rising linearly from $n_b = 0.0n_0$ to $4.0n_0$ over a length of $6920 \mu\text{m}$ after traveling a distance of $k_\beta s = 12.5$. The beam has undergone hosing after about the same distance as in Fig. 3. This beam is also compared with the numerical solutions in Fig. 4(c) and we find a much closer match than for the Gaussian pulse. Clearly, the more uniform channel agrees better with the theory, and reflects the fact that hosing is dependent on channel formation.

The previous simulations were done for parameters where the theory predicts only a few exponentiations of hosing growth. However, for future PWFA experiments, such as the “afterburner” [18] which attempts to at least double the energy of the driver, the predicted amount of hosing is much larger. For example, if a SLAC type bunch were compressed by a factor of ten, then its energy could be boosted to greater than 100 GeV in a distance ~ 10 m, using a plasma of density $\sim 2 \times 10^{16} \text{ cm}^{-3}$. For these parameters, $k_\beta L = 422$, and Eqs. (1) and (2) predict a factor of 10000 growth within only 2.5 m for a position $\omega_0 \xi = 3.75$ from the front of the beam. Even using the world's fastest computers it is still not possible to model such parameters using OSIRIS. Therefore, we use a recently developed parallelized quasistatic PIC code which solves the same basic equations as in Ref. [14], except we

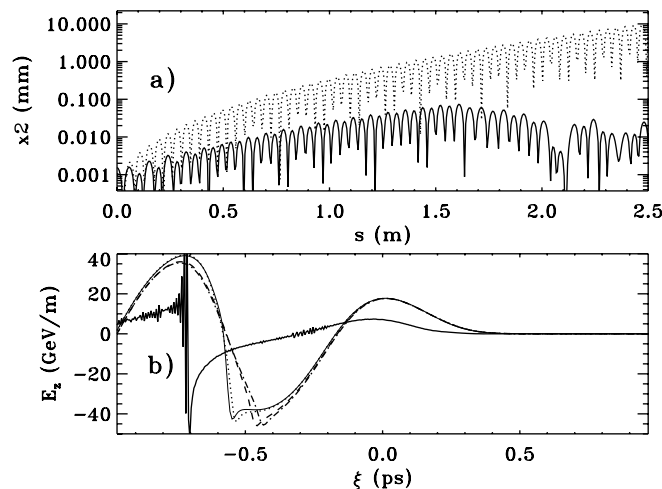


FIG. 5. The centroid of an afterburner simulation is plotted (solid) against the theoretical curve (dashed). Lineouts of the accelerating gradient are plotted for several different times. For comparison results from an OSIRIS simulation are also shown.

include relativistic mass corrections. These frozen field magnetoinductive equations are the starting point for hosing theory, and this code includes additional particle and short-pulse effects. We used a $256 \times 256 \times 256$ grid with a physical dimension $16c/\omega_p$ in each direction. There are 4 plasma particles per cell and 5 242 880 beam particles. The beam was centered in the middle of the box with a $\sigma_\xi = 45 \mu\text{m}$, and $\sigma_x = \sigma_y = 7 \mu\text{m}$, and had an initial linear tilt with $0.495 \mu\text{m}$ offset at σ_ξ . In Fig. 5(a), we plot the centroid of the beam vs propagation distance for both the simulation and the solutions to Eqs. (1) and (2) integrated back from the position of complete blowout, $3c/\omega_p$ in front of the peak. The centroid is taken at an axial position of $0.75c/\omega_p$ behind the pulse's peak.

Figure 5(a) clearly shows a smaller hosing growth rate in the simulation for $0 \leq s \leq 2.5$ m than is predicted by theory. Furthermore, the instability saturates when the beam hits the edge of the blowout region ($s \sim 2$ m), thus causing beam erosion. Although less severe than predicted by theory, hosing may still degrade the wake considerably. To study this we plot a line out of the accelerating field for $k_\beta s = 0, 62.4, 124.7, 187.1$ and we show a plot of the accelerating field from an OSIRIS run to show that the frozen field and magnetoinductive approximation is not as accurate as one might think. The differences are severe for these parameters because the plasma electrons acquire relativistic energies and substantial axial velocities. Figure 5(b) shows that the wake remains surprisingly stable for the length of the simulation. This indicates that hosing may not necessarily be devastating to the accelerating field but will be an important issue regarding overall efficiency. We have also plotted in Fig. 3(b) the results from the magnetoinductive code (dotted line) to show that it predicts more growth than OSIRIS. Therefore, the magnetoinductive code provides an upper bound for the hosing growth.

This PIC simulation study shows that hosing occurs differently for short pulses in which the ion channel is self-

generated nonadiabatically. The reason clearly lies in how the offset of the beam centroid creates an offset in the channel, i.e., the relative position of the null in the focusing force. In particular, Eqs. (1) and (2) are derived assuming a perfectly round channel equilibrium being rigidly displaced. For short pulses, this is not the case. First, the zeroth order solution is made of plasma electrons executing nonlinear trajectories, and hence it is difficult to determine how perturbations to these trajectories will behave. Second, the expelled electrons do not form an azimuthally symmetric sheath around the ion channel, and contribute to the focusing force as well. Obtaining a generalized theory for the hosing of short pulses is beyond the scope of this work, but the simulations presented here point out possible approaches. In particular, one needs to empirically find the relationship between the focusing force and beam offset to see how it changes with the amplitude of the offset. Furthermore, we have shown that the full set of Maxwell's equations, not just the magnetoinductive ones, are needed to accurately model future PWFA designs. Other areas for future work are the hosing of asymmetric and positron beams, which both lead to anharmonic character in the focusing forces of the channel.

We acknowledge useful conversations with the entire E-157 Collaboration and Dr. V.K. Decyk. Work was supported by DOE under Contracts No. DE-FG03-92ER40727 and No. DE-FG03-92ER40745, and by NSF Grants No. DMS-9722121, No. Phy-0078508, No. ECS-9617089, and No. 53-4502-7420. The OSIRIS simulations were run on the Cray T3E at NERSC.

-
- [1] J. B. Rosenzweig *et al.*, Phys. Rev. A **44**, R6189 (1991).
 - [2] D. H. Whittum *et al.*, Phys. Rev. Lett. **67**, 991 (1991).
 - [3] J. Krall and G. Joyce, Phys. Plasmas **2**, 1326 (1995).
 - [4] N. Barov *et al.*, Phys. Rev. ST Accel. Beams **3**, 011301 (2000).
 - [5] M. J. Hogan *et al.*, Phys. Plasmas **7**, 2241 (2000).
 - [6] H. L. Buchanan, Phys. Fluids **30**, 221 (1987).
 - [7] D. H. Whittum *et al.*, Phys. Rev. A **46**, 6684 (1992).
 - [8] M. Lampe *et al.*, Phys. Fluids B **5**, 1888 (1993).
 - [9] D. H. Whittum, Phys. Fluids B **5**, 4432 (1993).
 - [10] D. H. Whittum, Phys. Plasmas **4**, 1154 (1997).
 - [11] D. H. Whittum, J. Phys. D **30**, 2958 (1997).
 - [12] Y. Y. Lau, Phys. Rev. Lett. **63**, 1141 (1989).
 - [13] B. E. Blue, Masters thesis, University of California, Los Angeles, 2000.
 - [14] A. A. Geraci and D. H. Whittum, Phys. Plasmas **7**, 3431 (2000).
 - [15] W. B. Mori *et al.*, Part. Accel. **31**, 1229 (1990).
 - [16] R. G. Hemker *et al.*, in *Proceedings of the 1999 Particle Accelerator Conference, New York, 1999* (IEEE, Piscataway, NJ, 1999).
 - [17] P. Chen *et al.*, Phys. Rev. Lett. **56**, 1252 (1986).
 - [18] S. Lee *et al.*, Phys. Rev. ST Accel. Beams **5**, 011001 (2002).